Asymmetry in Polymer-Solvent Interactions Yields Complex Thermoresponsive Behavior

Satyen Dhamankar and Michael A. Webb*

Department of Chemical and Biological Engineering, Princeton University, Princeton, NJ, USA

E-mail: mawebb@princeton.ed

Abstract

We introduce a lattice framework that incorporates elements of Flory-Huggins solution theory and the q-state Potts model to study the phase behavior of polymer solutions and single-chain conformational characteristics. Without empirically introducing temperature-dependent interaction parameters, standard Flory-Huggins theory describes systems that are either homogeneous across temperatures or exhibit upper critical solution temperatures. The proposed Flory-Huggins-Potts framework extends these capabilities by predicting lower critical solution temperatures, miscibility loops, and hourglass-shaped spindle curves. We particularly show that including orientation-dependent interactions, specifically between monomer segments and solvent particles, is alone sufficient to observe such phase behavior. Signatures of emergent phase behavior are found in single-chain Monte Carlo simulations, which display heating- and cooling-induced coil-globule transitions linked to energy fluctuations. The framework also capably describes a range of experimental systems. Importantly, and by contrast to many prior theoretical approaches, the framework does not employ any temperature- or composition-dependent parameters. This work provides new insights regarding the microscopic physics that underpin complex thermoresponsive behavior in polymers.

Thermoresponsive polymers (TRPs) drastically alter structure, functionality, and/or stability upon changes in temperature.[1–3] They are appealing candidates for many applications, such as drug delivery, sensing, and purification.[4–12] Their physics also have implications for biological systems, with parallels to cold and warm denaturation of proteins, the hydrophobic effect, the formation of biomolecular condensates, and folding of DNA/RNA nanostructures.[13–22] Manipulating how polymer-based materials respond to temperature could also enhance control over supramolecular assemblies and improve particle engineering.[23–25] Consequently, understanding and modeling TRPs is of significant interest.

No self-contained theoretical framework currently captures the range of behaviors observed in TRPs. Flory-Huggins solution theory[26,27] (FH) is a simple conceptual starting point, but balancing short-ranged interactions against chain and solvent entropy only yields upper critical solution temperatures (UCST) and heating-induced globule-coil transitions (GCT).[26–29] Emergence of lower critical solution temperatures (LCST) or heating-induced coil-globule transitions (CGT) has been addressed by theoretical extensions,[30–45] which either introduce adjustable parameters or impose *ad hoc* temperature-dependence to existing ones. Some representative strategies include utilizing void sites and instituting surface-area effect corrections,[31] incorporating secondary lattices with temperature-dependent perturbative interactions,[42,44] invoking specific associative interactions,[46] or prescribing an equation of state.[34,44,45] Although these approaches are powerful and expressive, they often lack a firm microscopic basis, which inhibits validation, extension, interpretation, and application. By contrast, molecular simulation analysis has pointed to molecular size effects, hydrogen-bonding, and other orientation-dependent interactions as important for thermoresponsive behavior.[16,47–55] However, the chemical specificity obfuscates general comprehension and presents little opportunity to isolate the minimal and necessary set of interactions. Thus, questions remain regarding the microscopic physics of TRPs.

In this Letter, we introduce a minimal framework that combines elements of Flory-Huggins theory[26,27] and the q-states Potts model[56,57] to understand phase behavior and

the CGT in TRPs. A key feature of this Flory-Huggins-Potts (FHP) framework is that all model parameters are linked to a Hamiltonian that transparently depends on pairwise interaction energies amongst monomer and solvent particles. By consequence, derived models are free of temperature- and composition-dependent parameters, permitting both analytical analysis and commensurate investigation with molecular simulation. Mean-field analysis reveals that asymmetry in monomer-solvent interactions is alone sufficient to produce intricate phase behavior, such as miscibility loops and hourglass-shaped phase envelopes, which are not captured by native FH. Furthermore, Monte Carlo simulations establish a connection between anticipated phase behavior and single-chain conformational characteristics, which enables microscopic analysis that extends our mean-field understanding. The FHP framework is also shown to reproduce diverse phase-coexistence data for several experimental systems. These findings not only highlight energetic asymmetries as important physics underlying TRPs but also establish a self-contained, conceptual framework that may be broadly applied to TRPs or extended to other stimuli-responsive systems.

We consider a lattice completely occupied by either solvent particles or monomer segments (Fig. 1a). Like FH, short-ranged, pairwise interactions exist between particles, and polymers consist of bonded monomer segments. Like a q-state Potts model, particles possess orientations that can influence pairwise energies. The system energy is

$$\mathcal{H} = \overbrace{\frac{1}{2}\sum_{i=1}^{n}\sum_{j\in\mathcal{N}(i)}\varepsilon_{\mathrm{FHP}}\left(\alpha_i,\alpha_j,\hat{\sigma}_i,\hat{\sigma}_j\right)}^{\substack{\text{short-range,}\\ \text{orientation-dependent interactions}}} + \overbrace{\sum_{k=1}^{N_p}\sum_{l=1}^{N_m-1}V\left(\vec{r}_{l+1}^{(k)},\vec{r}_{l}^{(k)}\right)}^{\text{excluded volume}} \tag{1}$$

with

$$V\left(\vec{r}_{l+1}^{(k)},\vec{r}_{l}^{(k)}\right) = \begin{cases} 0 & \text{if } \left|\vec{r}_{l+1}^{(k)}-\vec{r}_{l}^{(k)}\right| \in \mathcal{N}(\mathcal{O}) \\ \infty & \text{otherwise} \end{cases} \tag{2}$$

where α_i denotes the species (monomer or solvent) and $\hat{\sigma}_i$ denotes the unit-vector orientation

of the the particle occupying the ith lattice site; $\varepsilon(\cdot)$ is a pairwise energy function of such variables; n is the total number of lattice sites; N_p is the number of polymer chains; N_m is the number of monomer segments per chain; $\mathcal{N}(i)$ denotes the "neighborhood" of the particle i; $\vec{r}_l^{(k)}$ is the position of the lth monomer segment in the kth polymer chain; and $V(\cdot)$ is a potential function that ensures bonded monomer segments are within the neighborhood of each other. On a simple cubic lattice, we consider the neighborhood of the origin $\mathcal{N}(\mathcal{O})$ to consist of nearest, next-nearest, and next-next-nearest neighboring positions on the lattice, which results in a coordination number of $z = 26$.

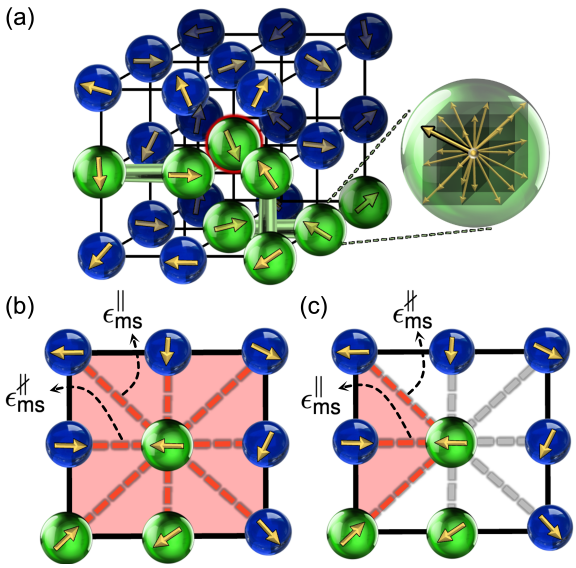

Figure 1: Schematic of the Flory-Huggins-Potts framework. (a) The local neighborhood of a site (red outline) for a simple cubic lattice. Monomer (m) segments and bonds are in green, and solvent particles (s) are blue. (b, c) Two-dimensional illustrations of possible manifestations of orientation-dependent interactions. In (b), aligned interactions are permitted with all neighboring particles, which may capture physics akin to hydrogen-bond networks. In (c), aligned interactions are permitted with only a subset of neighboring particles, which may reflect specific and exclusive associative interactions. In both panels, particles adjoined by red lines in the shaded region can engage in aligned ($\parallel$) interactions; those adjoined by gray only exhibit misaligned ($\nparallel$) interactions.

To simplify, we decompose

$$\varepsilon(\alpha_i, \alpha_j, \hat{\sigma}_i, \hat{\sigma}_j) = \epsilon^{\nparallel}_{\alpha_i\alpha_j} + \Lambda(i,j)\Delta_{\alpha_i\alpha_j} \tag{3}$$

where $\Delta_{\alpha_i\alpha_j} = \epsilon^{\parallel}_{\alpha_i\alpha_j} - \epsilon^{\nparallel}_{\alpha_i\alpha_j}$ quantifies an asymmetry or difference for interactions between species α_i and α_j in an "aligned" ($\parallel$) versus "misaligned" ($\nparallel$) state, and misaligned and aligned states are effectively set by a function $\Lambda(i,j) \in [0,1]$. By convention, we presume

that $\Delta_{\alpha_i\alpha_j} \leq 0$, such that that aligned interactions are energetically more favorable than misaligned ones, if present. We envision that both $\Delta_{\alpha_i\alpha_j}$ and $\Lambda(i,j)$ capture essential differences in how particles (or groups thereof) may interact (e.g., due to preferred molecular orientations or collective arrangements that constitute solvation motifs). Under this interpretation, the FHP framework is an effective coarse-grained representation of the system, for which each particle on a lattice site may represent one or many molecules, and the associated orientations represent a collective behavior or configurational rearrangement the molecules comprising the particle on that lattice site. Therefore, despite Eq. 1 featuring only pairwise terms, $\varepsilon_{\mathrm{FHP}}\left(\alpha_i, \alpha_j, \hat{\sigma}_i, \hat{\sigma}_j\right)$ can approximate more complex many-body interactions through the dependence on $\hat{\sigma}_i$ and $\hat{\sigma}_j$.

For concreteness, we suggest two physically motivated manifestations of Λ, colloquially referenced as correlation networks (Fig. 1b) and locking interactions (Fig. 1c). Inspired by hydrogen-bonding networks,[58] correlation-networks use

$$\Lambda_{\mathrm{corr}}(i,j) = \Theta(\hat{\sigma}_i \cdot \hat{\sigma}_j - \delta), \tag{4}$$

and inspired by specific associative interactions[59,60] (e.g., hydrogen-bonding, metal–ligand, screened electrostatics, or perhaps short-ranged dipole-dipole or π-π stacking), locking interactions use

$$\Lambda_{\mathrm{lock}}(i,j) = \Theta(\delta - [\arccos\left(\hat{r}_{ji} \cdot \hat{\sigma}_i\right) + \arccos\left(\hat{r}_{ij} \cdot \hat{\sigma}_j\right)]) \tag{5}$$

where $\hat{r}_{ij} = \frac{\vec{r}_i - \vec{r}_j}{|\vec{r}_i - \vec{r}_j|}$. In both Eqs. (4) and (5), $\Theta(\cdot)$ denotes a Heaviside step function, such that δ effectively determines a solid angle through which particle orientations are considered aligned. A primary distinction between Λ_{corr} and Λ_{lock} is the fraction of neighboring particles capable of engaging in aligned interactions, denoted p_v. For Λ_{corr}, aligned interactions occur when particle orientations have the same direction (within the specified threshold δ), allowing all neighboring particles to participate without restrictions. Conversely, for Λ_{lock}, aligned interactions require particle orientations to be directed towards the other particle, which

limits possiblly aligned interactions to only a subset of neighboring particles. Therefore, $p_v = 1$ for Λ_{corr}, while $p_v \leq 1$ for Λ_{lock} (see Figs. 1b,c). We note that there are many reasonable choices for expressing interaction asymmetry, and FHP is not exclusive to Eqs. (4) and (5). Furthermore, FHP reduces to a simple FH description in the limit that all $\Delta_{\alpha_i\alpha_j} = 0$, and one can simply write $\epsilon_{\alpha_i\alpha_j}$ with no need to distinguish misaligned and aligned interactions.

Following principles of FH and Boltzmann statistics (Supplemental Information, Section S1), the free energy of mixing per particle is

$$\frac{\Delta \bar{F}_{\mathrm{mix}}}{k_{\mathrm{B}}T} = \overbrace{\chi_{\mathrm{FHP}}(T)\,\varphi(1-\varphi)}^{\text{energetic term}} + \overbrace{\frac{\varphi}{N_m v_m}\ln\varphi + \frac{(1-\varphi)}{v_s}\ln(1-\varphi)}^{\text{entropic term}} \tag{6}$$

where φ is the volume fraction of the polymer, N_m is the degree of polymerization, v_m is the molar volume of a monomer segment, and v_s is the same for a solvent molecule (or group thereof). Furthermore,

$$\chi_{\mathrm{FHP}}(T) \equiv \chi_{\mathrm{FH}}(T) + \tilde{\chi}(T) \tag{7}$$

where

$$\chi_{\mathrm{FH}}(T) \equiv \frac{(z-2)}{k_{\mathrm{B}}T}\left(\epsilon^{\nparallel}_{\mathrm{ms}} - \frac{1}{2}\left(\epsilon^{\nparallel}_{\mathrm{mm}} + \epsilon^{\nparallel}_{\mathrm{ss}}\right)\right) \tag{8}$$

is essentially equivalent to a FH interaction parameter for a lattice with coordination number z and pairwise energies set at the misaligned energy scale, and

$$\tilde{\chi}(T) \equiv \frac{(z-2)}{k_{\mathrm{B}}T} p_v \left(\tilde{\Delta}_{\mathrm{ms}}(T) - \frac{1}{2}\left(\tilde{\Delta}_{\mathrm{mm}}(T) + \tilde{\Delta}_{\mathrm{ss}}(T)\right)\right) \tag{9}$$

accounts for asymmetry between aligned and misaligned interactions and their relative prevalence. In particular, the $\tilde{\Delta}_{ij}$ terms amount to per-site free-energy corrections between aligned

and misaligned states given by

$$\tilde{\Delta}_{ij}(T) = \frac{\Delta_{ij}}{1 + \left(\frac{1-p_\Omega}{p_\Omega}\right) \exp\left(\Delta_{ij}/k_\mathrm{B}T\right)} \tag{10}$$

where p_Ω is the fraction of states that lead to aligned interaction between two particles that can engage in aligned interactions. p_Ω and p_v can be evaluated with numerically for particles on a lattice.

Eq. 6 itself is functionally analogous to the FH free energy of mixing, yet Eqs. (7)-(10) seemingly introduce five parameters beyond FH ($\Delta_\mathrm{ms}, \Delta_\mathrm{ss}, \Delta_\mathrm{mm}, p_\Omega, p_v$) belying simplicity. However, neither p_v nor r are "free" parameters as they directly relate to the physical interactions (i.e., what constitutes aligned vs. misaligned) and follow from a defined Hamiltonian. This potentially leaves twice as many energy parameters compared to original FH. However, we will show that a minimal model to observe complex phase behavior only requires $\Delta_\mathrm{ms} < 0$ (with p_v and p_Ω as nonzero).

To illustrate, we characterize the phase behavior for a select set of models from four FHP-derived regimes. In FHP, we anticipate four regimes of qualitatively distinct $\chi_\mathrm{FHP}(T)$ behavior – denoted as $\mathcal{R}_0$, $\mathcal{R}'_1$, $\mathcal{R}_2$, or $\mathcal{R}'_3$ (Fig. 2a) – that determine observed phases. The notation is such that the subscript indicates the number of homogeneous-to-phase-separated transitions, a prime ($'$) indicates a phase-separated state at low T, and no prime indicates a homogeneous state at low T. The spinodals in Fig. 2b illustrate how the FHP framework exhibits complex phase behavior relative to FH for specific parameter-sets representative of $\mathcal{R}'_1$, $\mathcal{R}_2$, and $\mathcal{R}'_3$. While $\mathcal{R}'_1$ displays the standard UCST, $\mathcal{R}_2$ and $\mathcal{R}'_3$ respectively display a miscibility loop and an hourglass-like phase envelope, which is usually recovered by invoking an equation-of-state or otherwise presuming temperature-dependent parameters. These models use $\Delta_\mathrm{mm} = \Delta_\mathrm{ss} = 0$, which suggests that introducing interaction asymmetry to monomer-solvent interactions $\epsilon^{\parallel}_\mathrm{ms} < \epsilon^{\nparallel}_\mathrm{ms}$ is alone sufficient to obtain miscibility loops and hourglass-like phase envelopes.

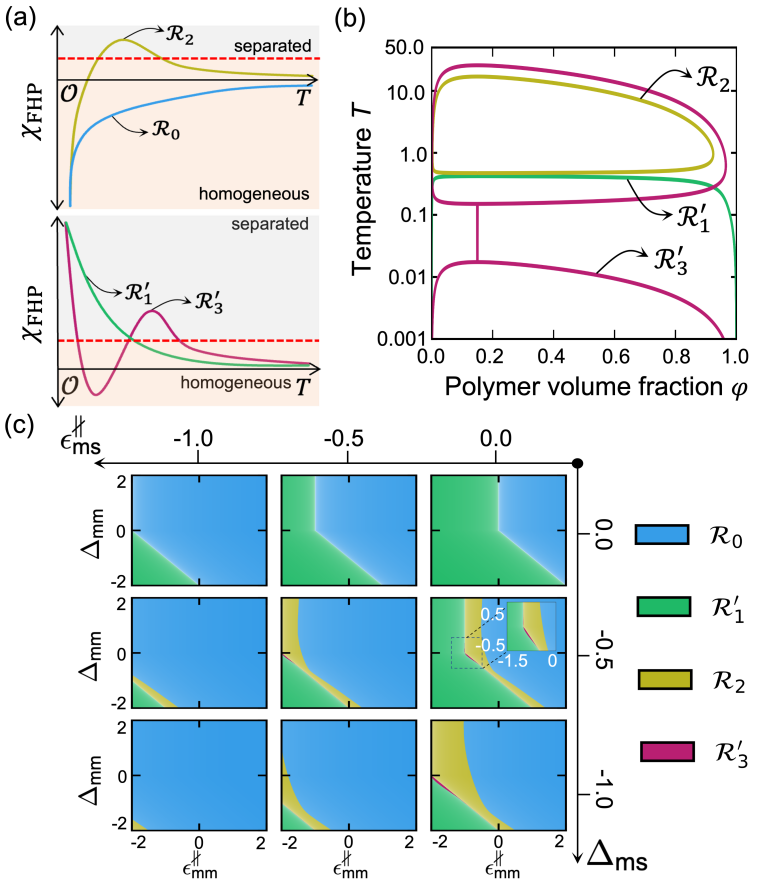

Figure 2: Phase behavior of polymer solutions described by the Flory-Huggins-Potts framework. Representative temperature-volume fraction ($T-\varphi$) for a polymer with degree of polymerization $N_m = 32$, monomer molar volume $v_m = 1$ and solvent molar volume $v_s = 1$. (a) Qualitative examples of $\chi_{\mathrm{FHP}}(T)$ for classification of phase behavior. Systems from $\mathcal{R}_0$ are expected to be homogeneous, while those from $\mathcal{R}'_1$, $\mathcal{R}_2$, and $\mathcal{R}'_3$ respectively feature upper critical solution temperatures, miscibility loops, and hourglass-shaped phase envelopes. (b) Spinodal curves on temperature-volume fraction ($T-\varphi$) diagrams for models by fixing all other parameters as $(\epsilon^{\sharp}_{\mathrm{ms}}, \Delta_{\mathrm{mm}}, \epsilon^{\sharp}_{\mathrm{mm}}, \Delta_{\mathrm{ss}}, \epsilon^{\sharp}_{\mathrm{ss}}, p_v, p_\Omega) = (0, -1, -1, 0, 0, 1, 0.5)$ and $z = 26$ and varying $\epsilon^{\parallel}_{\mathrm{ms}}$: $\mathcal{R}'_1$ ($\Delta_{\mathrm{ms}} = 0$), $\mathcal{R}_2$ ($\Delta_{\mathrm{ms}} = -1$), and $\mathcal{R}'_3$ ($\Delta_{\mathrm{ms}} = -0.5237$); parameters for $\mathcal{R}_0$ do not yield phase separation. (c) Classification of phase behavior as a function of $\epsilon^{\parallel}_{\mathrm{mm}}$ and $\epsilon^{\sharp}_{\mathrm{mm}}$ (inner plots) at various values of $\epsilon^{\parallel}_{\mathrm{ms}}$ and $\epsilon^{\sharp}_{\mathrm{ms}}$ (outer axes). Additional parameter-sets are examined in Supplemental Information (Figs. S1, S2).

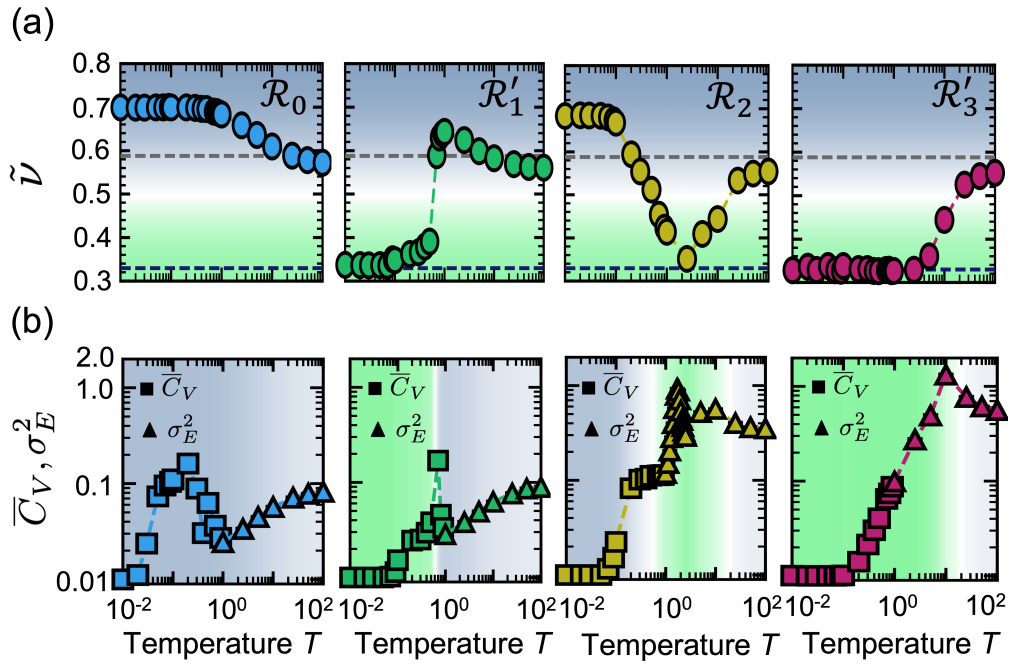

Figure 3: Analysis of single-chain Monte Carlo simulations. (a,b) Temperature dependence of (a) intra-chain scaling exponent $\tilde{\nu}$ and (b) energy fluctuations using parameters associated with $\mathcal{R}_0$, $\mathcal{R}'_1$, $\mathcal{R}_2$ and $\mathcal{R}'_3$ with $(\Delta_{\rm ss}, \epsilon^{\nparallel}_{\rm ss}, p_v, p_\Omega) = (0, 0, 1, 0.25)$ for all simulations. In (a), the horizontal dashed lines are guides to the eye for globular scaling (black) and excluded-volume statistics (gray). In (b), the data transitions such that heat capacity $\overline{C}_V$ is shown for $T < 1.0$ and fluctuations in total energy σ_E^2 is shown for $T \geq 1.0$; the data are shifted by 0.01 to allow for logarithmic scaling. The background color is based on $\tilde{\nu}$ to emphasize conformations that are expanded (blue) or globular (green) relative to the ideal chain (white). Simulation parameters $(\Delta_{\rm ms}, \epsilon^{\nparallel}_{\rm ms}, \Delta_{\rm mm}, \epsilon^{\nparallel}_{\rm mm})$ for $\mathcal{R}_0$ are $(0, -1, 0, -1)$, for $\mathcal{R}'_1$ are $(0, -1, -1.2, -1)$, for $\mathcal{R}_2$ are $(-1, 0, -1, -1)$, for $\mathcal{R}'_3$ are $(-1, 0, 0, -2.001)$. Error bars are smaller than the symbol size.

Conversely, only introducing asymmetry to monomer-monomer interactions (or likewise solvent-solvent) does not result in as rich phase behavior. This is conveyed in Fig. 2c, which provides a "hyperphase diagram" summarizing $\chi_{\rm FHP}(T)$ behavior across a much broader parameter-space rather as opposed to the select cases in Fig. 2b. While the preponderance of parameter-space yields $\mathcal{R}_0$ (blue) or $\mathcal{R}'_1$ (green) behavior, $\mathcal{R}_2$ (miscibility loops, yellow) and $\mathcal{R}'_3$ (hourglass envelopes, magenta) emerge within intermediate energetic regimes only if misaligned and aligned monomer-solvent interactions are unequal. Overall, these results show how the balance of both interspecies and intraspecies interactions as well as misaligned and aligned interactions give rise to nuanced phase behavior, but asymmetric interactions between monomer and solvent are essential to observe multiple phase transitions within the FHP framework.

Because the parameters within FHP are traceable to a well-defined Hamiltonian, molec-

ular simulation can be used to ascertain any connection between single-chain structure and solution thermodynamics.[51,61] Monte Carlo (MC) simulations are used to characterize the temperature-dependent behavior of single polymer chains using parameters from each of $\mathcal{R}_0$, $\mathcal{R}_1'$, $\mathcal{R}_2$, and $\mathcal{R}_3'$. The simulations use $N_m = 32$ and a Λ_{corr} with $p_v = 1$ and for $\delta = \cos 1$ gives $p_\Omega = 0.25$ (see Fig. 1b). To probe single-chain conformations, we extract intra-chain scaling exponents $\tilde{\nu}$ by fitting data

$$\left\langle |\vec{r}_i - \vec{r}_j|^2 \right\rangle \propto |i-j|^{2\tilde{\nu}} \tag{11}$$

and compare with known scaling laws (e.g., $R_{\text{g}} \propto M^{1/2}$ for ideal chains, $R_{\text{g}} \propto M^{1/3}$ for globules); the finite-size of our chains motivates fitting data over a selected range of separation distances (see Supplemental Information, Figure S2).

Fig. 3a shows that distinct single-chain conformational behavior is observed when parameters are taken from different phase behavior regimes. At low T, systems from $\mathcal{R}_0$ and $\mathcal{R}_2$ with strong aligned monomer-solvent interactions exhibit scaling indicative of good-solvent conditions ($\tilde{\nu} \geq 2/3$), while systems from $\mathcal{R}_1'$ and $\mathcal{R}_3'$ display more globular scaling; this correlates with $\mathcal{R}_0$ and $\mathcal{R}_2$ having a single homogeneous phase and $\mathcal{R}_1'$ and $\mathcal{R}_3'$ featuring phase-separated states. Behavior between $\mathcal{R}_0$ and $\mathcal{R}_2$ differs upon heating. While $\tilde{\nu}$ from $\mathcal{R}_0$ gradually approaches excluded-volume statistics ($\tilde{\nu} \sim 0.588$), $\tilde{\nu}$ from $\mathcal{R}_2$ collapses to a globule before expanding in the high-T limit, which aligns with the physics of a miscibility loop. Similar explanations apply for $\mathcal{R}_1'$ and $\mathcal{R}_3'$. The singular GCT for $\tilde{\nu}$ from $\mathcal{R}_1'$ with asymmetric monomer-monomer interactions is consistent with a UCST, but a sharp transition is only observed with sufficiently asymmetric interactions. For $\mathcal{R}_3'$, there is no clear mapping of the $\tilde{\nu}$ behavior to the solution phase behavior. $\tilde{\nu}$ shows globular behavior at low temperatures and maintains the globular state while allowing for energetic fluctuations in the system before eventually expanding. ~~For $\mathcal{R}_3'$, $\tilde{\nu}$ begins as globular then crosses the ideal-chain limit three times–a progression consistent with an hourglass-like phase enve-~~

~~lope.~~ In contrast, $\tilde{\nu}$ obtained with isotropic interactions, which comports to simple FH, only tends gradually and monotonically to excluded-volume statistics upon heating (Supplemental Information, Fig. S3). Thus, anisotropic interactions can drive sharp, thermally induced conformational transitions – reminiscent of the trends seen in phase behavior.

The observed conformational transitions are also accompanied by drastic shifts in underlying energy fluctuations (Fig. 3b). For systems from $\mathcal{R}_1'$, the single CGT is marked by maxima in the heat capacity $\overline{C}_V$ and energy fluctuations σ_E^2 within a narrow temperature range wherein $\tilde{\nu} \sim 0.5$ (white region); similar observations hold for the low-T CGT in $\mathcal{R}_2$. Such behavior is reminiscent of typical second-order Θ transitions of polymer chains,[48] although firm elucidation is left to future work. In $\mathcal{R}_2$ and $\mathcal{R}_3'$, a higher-T transition from globular to excluded-volume statistics is captured by a maximum in σ_E^2. These fluctuations notably accompany compositional and orientational changes within the polymer's local environment (Supplemental Information, Figs. S2 and S3) and are thus not reproducible by FH but are inherent to FHP.

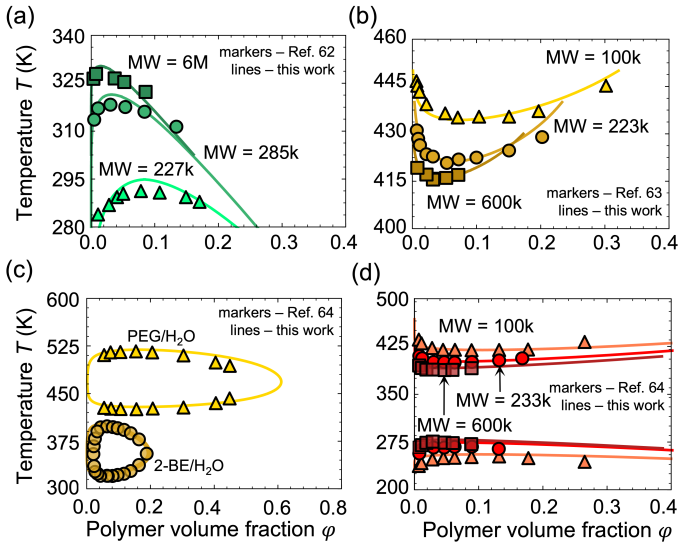

Figure 4: Comparison to experimental coexistence data for diverse systems. Temperature-volume fraction ($T - \phi$) diagrams for systems that display (a) upper critical solution temperatures, such as polyisbutylene (PIB) in diisobutyl ketone at several molecular weights (MW); (b) lower critical solution temperatures, such as polystyrene in ethyl acetate at several MW; (c) miscibility loops, such as polyethylene glycol (PEG) (3350 amu) in water and 2-butoxyethanol (2-BE) in water; and (d) hourlgass-like phase behavior, such as polystyrene in tert-butyl acetate at several MW. The data in (a)-(d) are respectively sourced from Refs.,[62],[63] and[64] and were also compared to theory proposed in Ref.[42,65] All molecular weights are reported in Daltons. All parameters are reported in the Supplemental Information (Table 4).

Finally, the FHP framework can quantitatively capture the behavior of experimental sys-

tems. This is illustrated in Fig. 4, which compares FHP results with experimental data for various solutions that collectively showcase UCST, LCST, miscibility loops, and hourglass (UCST + LCST) phase envelopes. These same systems were examined by Bae and Oh to evaluate a proposed double-lattice model.[63] Here, for each set of experimental data, the FHP parameters were optimized using the covariance matrix adaptation evolutionary strategy[66] with a procedure described in the Supplemental Information. It is notable that FHP captures the experimental data well without any temperature-dependent parameters or externally imposed equation-of-state, which is distinct from similarly expressive prior theoretical works.[32,44,63] The reproduction of a lower-critical solution temperature (Fig. 4b) arises from parameters that yield miscibility loops, with the upper transition to a homogenous phase occurring at high temperatures. We emphasize that the parameters obtained are not unique, which obfuscates their physical interpretation, but there is consistency with certain reasonable expectations. For example, for a specified materials system, the underlying energetic parameters are roughly constant while terms accounting for the molar volume of components tend to increase with increasing molecular weights. Although the quality of fits here does not firmly exclude the importance of other key interactions, the restriction that parameters be represented in a well-defined Hamiltonian (and subsequent free-energy expressions) implies that parameter-space of FHP does not have arbitrary flexibility to represent complex functions. Consequently, effectively capturing experimental data is not only an important demonstration for FHP but bolsters the case that energetic asymmetries, which distinguish FHP, are likely important to the physics of real systems.

In conclusion, we have introduced the Flory-Huggins-Potts (FHP) framework to describe and understand thermoresponsive polymers. Remarkably, this approach, which simply extends Flory-Huggins (FH) theory with orientation-dependent interactions, showcases diverse temperature-dependent phase behavior, including miscibility loops and hourglass-like phase envelopes. In this way, FHP can capture the experimental data of diverse systems. This expressive capacity emerges without any *ad hoc* functional dependencies on temperature;

the effects are transparently attributable to microscopic theory of interactions. Here, this enabled investigation of how polymer solution thermodynamics connect to single-chain conformational behavior. We find overall strong correspondence between single-chain conformational behavior (from molecular simulation) and macroscopic phase transitions (deduced from mean-field analysis), except that simulations for parameters that macroscopically produce hourglass-shaped phase envelopes do not produce multiple GCT upon heating. Importantly, while FHP supports additional complexity, a key result is that the emergence of complex phase behavior only requires $\Delta_{\mathrm{ms}} < 0$ (with p_v and p_Ω as nonzero). From analyzing such minimal models, we conclude that asymmetry in inter-species (e.g., monomer-solvent, as opposed to monomer-monomer and solvent-solvent) interactions is alone sufficient to induce complex thermoresponsive behavior, such as heating-induced CGT. It is important to note that this does not necessarily imply that such interactions are the sole cause or even predominant factor driving such phenomena in any specific chemically realistic system; however, the fact that the Hamiltonian underlying FHP can be parameterized to fit several distinct sets of experimental data is perhaps suggestive of its relevance.

FHP may be extended, tested, and applied in a variety of ways. Firstly, FHP models may serve as foundational scaffolding for other stimuli-responsive behaviors grounded in similar physical principles. For example, interaction asymmetry could impact the manifestation of cononsolvency, which is often observed for thermoresponsive polymers.[?] Classification of conformational transitions with FHP models is also of interest. Prior work has shown a first-order collapse transition with respect to a parameter governing the energy difference between a effectively solvated and non-solvated state for a polymer chain;[48] FHP models may produce similar behavior. Secondly, the simplicity and transparency of FHP physics make it suitable for benchmarking and hypothesis testing. Bottom-up coarse-graining of thermoresponsive polymers is challenged by state-point-dependent parameterization and generally complicated many-body molecular physics present in atomistic simulations.[55,67,68] FHP models could provide a useful benchmark system with requisite complexity but precisely known

physics. Thirdly, the FHP framework would benefit from firmer connection to the physics of chemically realistic systems. Because the parameters in FHP comport to a well-defined Hamiltonian, it may be feasible to extract parameters from calculations with molecular simulation (e.g., by evaluating energy or free-energy differences between interacting groups at different orientations).[?] Experimentally, one might examine whether the effects of certain chemical modifications are consistent with changes in thermoresponsive behavior expected from FHP according to anticipated effects on interaction asymmetries. These efforts could usefully support FHP as a viable theory for certain systems, such as phase-separating disordered proteins and RNAs.[69–71] Finally, FHP can facilitate interpretation of results within a hierarchy of models. If data cannot be viably fit to an FHP model, one may infer that additional physics beyond those captured by the FHP Hamiltonian underlie the system behavior. Achieving quantitative consistency may ultimately require extensions to consider neglected factors, such as compressibility, which has been considered elsewhere.

Acknowledgement

S.D. and M.A.W. acknowledge support from the National Science Foundation under Grant No. 2237470. Simulations were performed using resources from Princeton Research Computing at Princeton University, which is a consortium led by the Princeton Institute for Computational Science and Engineering (PICSciE) and Office of Information Technology's Research Computing.

Supporting Information

Derivation of the mean field free energy. Example Hamiltonians. Representative phase behavior for distinct p_v and p_Ω. Monte Carlo simulation details. Characterization of monomer solvation environment. Comparison of critical temperatures to single-chain transition markers. Parameters to reproduce experimental coexistence curves.

References

(1) Karimi, M.; Zangabad, P. S.; Ghasemi, A.; Amiri, M.; Bahrami, M.; Malekzad, H.; Asl, H. G.; Mahdieh, Z.; Bozorgomid, M.; Ghasemi, A.; Boyuk, M. R. R. T.; Hamblin, M. R. Temperature-Responsive Smart Nanocarriers for Delivery Of Therapeutic Agents: Applications and Recent Advances. *ACS Applied Materials & Interfaces* **2016**, *8*, 21107–21133, DOI: 10.1021/acsami.6b00371.

(2) Kim, Y.-J.; Matsunaga, Y. T. Thermo-responsive polymers and their application as smart biomaterials. *Journal of Materials Chemistry B* **2017**, *5*, 4307–4321, DOI: 10.1039/c7tb00157f.

(3) Ward, M. A.; Georgiou, T. K. Thermoresponsive Polymers for Biomedical Applications. *Polymers* **2011**, *3*, 1215–1242, DOI: 10.3390/polym3031215.

(4) Davis, D. A.; Hamilton, A.; Yang, J.; Cremar, L. D.; Gough, D. V.; Potisek, S. L.; Ong, M. T.; Braun, P. V.; Martínez, T. J.; White, S. R.; Moore, J. S.; Sottos, N. R. Force-induced activation of covalent bonds in mechanoresponsive polymeric materials. *Nature* **2009**, *459*, 68–72, DOI: 10.1038/nature07970.

(5) Colson, Y. L.; Grinstaff, M. W. Biologically Responsive Polymeric Nanoparticles for Drug Delivery. *Advanced Materials* **2012**, *24*, 3878–3886, DOI: 10.1002/adma.201200420.

(6) Tanaka, T.; Nishio, I.; Sun, S.-T.; Ueno-Nishio, S. Collapse of Gels in an Electric Field. *Science* **1982**, *218*, 467–469, DOI: 10.1126/science.218.4571.467.

(7) Thévenot, J.; Oliveira, H.; Sandre, O.; Lecommandoux, S. Magnetic responsive polymer composite materials. *Chemical Society Reviews* **2013**, *42*, 7099, DOI: 10.1039/c3cs60058k.

(8) Zhai, L. Stimuli-responsive polymer films. *Chemical Society Reviews* **2013**, *42*, 7148, DOI: 10.1039/c3cs60023h.

(9) Mukherji, D.; Watson, M. D.; Morsbach, S.; Schmutz, M.; Wagner, M.; Marques, C. M.; Kremer, K. Soft and Smart: Co-nonsolvency-Based Design of Multiresponsive Copolymers. *Macromolecules* **2019**, *52*, 3471–3478, DOI: 10.1021/acs.macromol.9b00414.

(10) Stuart, M. A. C.; Huck, W. T. S.; Genzer, J.; Müller, M.; Ober, C.; Stamm, M.; Sukhorukov, G. B.; Szleifer, I.; Tsukruk, V. V.; Urban, M.; Winnik, F.; Zauscher, S.; Luzinov, I.; Minko, S. Emerging applications of stimuli-responsive polymer materials. *Nature Materials* **2010**, *9*, 101–113, DOI: 10.1038/nmat2614.

(11) Mukherji, D.; Marques, C. M.; Kremer, K. Smart Responsive Polymers: Fundamentals and Design Principles. *Annual Review of Condensed Matter Physics* **2020**, *11*, 271–299, DOI: 10.1146/annurev-conmatphys-031119-050618.

(12) Xu, X.; Bizmark, N.; Christie, K. S. S.; Datta, S. S.; Ren, Z. J.; Priestley, R. D. Thermoresponsive Polymers for Water Treatment and Collection. *Macromolecules* **2022**, *55*, 1894–1909, DOI: 10.1021/acs.macromol.1c01502.

(13) Zeng, X.; Holehouse, A. S.; Chilkoti, A.; Mittag, T.; Pappu, R. V. Connecting Coil-to-Globule Transitions to Full Phase Diagrams for Intrinsically Disordered Proteins. *Biophysical Journal* **2020**, *119*, 402–418, DOI: 10.1016/j.bpj.2020.06.014.

(14) Scarpa, J. S.; Mueller, D. D.; Klotz, I. M. Slow hydrogen-deuterium exchange in a non-.alpha.-helical polyamide. *Journal of the American Chemical Society* **1967**, *89*, 6024–6030, DOI: 10.1021/ja01000a006.

(15) Shakhnovich, E. I.; Finkelstein, A. V. Theory of cooperative transitions in protein molecules. I. Why denaturation of globular protein is a first-order phase transition. *Biopolymers* **1989**, *28*, 1667–1680, DOI: 10.1002/bip.360281003.

(16) de los Rios, P.; Caldarelli, G. Putting proteins back into water. *Physical Review E* **2000**, *62*, 8449–8452, DOI: 10.1103/physreve.62.8449.

(17) Gelbart, W. M.; Bruinsma, R. F.; Pincus, P. A.; Parsegian, V. A. DNA-Inspired Electrostatics. *Physics Today* **2000**, *53*, 38–44, DOI: 10.1063/1.1325230.

(18) Shin, Y.; Brangwynne, C. P. Liquid phase condensation in cell physiology and disease. *Science* **2017**, *357*, DOI: 10.1126/science.aaf4382.

(19) Dignon, G. L.; Zheng, W.; Kim, Y. C.; Mittal, J. Temperature-Controlled Liquid–Liquid Phase Separation of Disordered Proteins. *ACS Central Science* **2019**, *5*, 821–830, DOI: 10.1021/acscentsci.9b00102.

(20) Geary, C.; Rothemund, P. W. K.; Andersen, E. S. A single-stranded architecture for cotranscriptional folding of RNA nanostructures. *Science* **2014**, *345*, 799–804, DOI: 10.1126/science.1253920.

(21) Han, D.; Qi, X.; Myhrvold, C.; Wang, B.; Dai, M.; Jiang, S.; Bates, M.; Liu, Y.; An, B.; Zhang, F.; Yan, H.; Yin, P. Single-stranded DNA and RNA origami. *Science* **2017**, *358*, DOI: 10.1126/science.aao2648.

(22) Jia, Y.; Chen, L.; Liu, J.; Li, W.; Gu, H. DNA-catalyzed efficient production of single-stranded DNA nanostructures. *Chem* **2021**, *7*, 959–981, DOI: 10.1016/j.chempr.2020.12.001.

(23) Yoo, J.-W.; Mitragotri, S. Polymer particles that switch shape in response to a stimulus. *Proceedings of the National Academy of Sciences* **2010**, *107*, 11205–11210, DOI: 10.1073/pnas.1000346107.

(24) Lewandowski, W.; Fruhnert, M.; Mieczkowski, J.; Rockstuhl, C.; Górecka, E. Dynamically self-assembled silver nanoparticles as a thermally tunable metamaterial. *Nature Communications* **2015**, *6*, DOI: 10.1038/ncomms7590.

(25) Bupathy, A.; Frenkel, D.; Sastry, S. Temperature protocols to guide selective self-assembly of competing structures. *Proceedings of the National Academy of Sciences* **2022**, *119*, DOI: 10.1073/pnas.2119315119.

(26) Flory, P. J. The Configuration of Real Polymer Chains. *The Journal of Chemical Physics* **1949**, *17*, 303–310, DOI: 10.1063/1.1747243.

(27) Flory, P. J. *Principles of polymer chemistry*; Ithaca, NY, Cornell University Press, 1953., 1953.

(28) de Gennes, P. G. *Scaling Concepts in Polymer Physics*; Cornell University Press, 1979.

(29) Gennes, P. D. Collapse of a polymer chain in poor solvents. *Journal de Physique Lettres* **1975**, *36*, 55–57, DOI: 10.1051/jphyslet:0197500360305500.

(30) Lacombe, R. H.; Sanchez, I. C. Statistical thermodynamics of fluid mixtures. *The Journal of Physical Chemistry* **1976**, *80*, 2568–2580, DOI: 10.1021/j100564a009.

(31) Sanchez, I. C.; Lacombe, R. H. An elementary molecular theory of classical fluids. Pure fluids. *The Journal of Physical Chemistry* **1976**, *80*, 2352–2362, DOI: 10.1021/j100562a008.

(32) Sanchez, I. C.; Lacombe, R. H. Statistical Thermodynamics of Polymer Solutions. *Macromolecules* **1978**, *11*, 1145–1156, DOI: 10.1021/ma60066a017.

(33) Panayiotou, C. G. Lattice-fluid theory of polymer solutions. *Macromolecules* **1987**, *20*, 861–871, DOI: 10.1021/ma00170a026.

(34) Panayiotou, C.; Sanchez, I. C. Hydrogen bonding in fluids: an equation-of-state approach. *The Journal of Physical Chemistry* **1991**, *95*, 10090–10097, DOI: 10.1021/j100177a086.

(35) Veytsman, B. A. Are lattice models valid for fluids with hydrogen bonds? *The Journal of Physical Chemistry* **1990**, *94*, 8499–8500, DOI: 10.1021/j100386a002.

(36) Simmons, D. S.; Sanchez, I. C. A Model for a Thermally Induced Polymer Coil-to-Globule Transition. *Macromolecules* **2008**, *41*, 5885–5889, DOI: 10.1021/ma800151p.

(37) Simmons, D. S.; Sanchez, I. C. Pressure Effects on Polymer Coil-Globule Transitions near an LCST. *Macromolecules* **2010**, *43*, 1571–1574, DOI: 10.1021/ma901485y.

(38) Dahanayake, R.; Dormidontova, E. Hydrogen Bonding Sequence Directed Coil-Globule Transition in Water Soluble Thermoresponsive Polymers. *Physical Review Letters* **2021**, *127*, 167801, DOI: 10.1103/physrevlett.127.167801.

(39) Matsuyama, A.; Tanaka, F. Theory of solvation-induced reentrant phase separation in polymer solutions. *Physical Review Letters* **1990**, *65*, 341–344, DOI: 10.1103/physrevlett.65.341.

(40) Bekiranov, S.; Bruinsma, R.; Pincus, P. Solution behavior of polyethylene oxide in water as a function of temperature and pressure. *Physical Review E* **1997**, *55*, 577–585, DOI: 10.1103/physreve.55.577.

(41) Choi, J.-M.; Dar, F.; Pappu, R. V. LASSI: A lattice model for simulating phase transitions of multivalent proteins. *PLOS Computational Biology* **2019**, *15*, e1007028, DOI: 10.1371/journal.pcbi.1007028.

(42) Oh, S. Y.; Bae, Y. C. Closed miscibility loop phase behavior of polymer solutions. *Polymer* **2008**, *49*, 4469–4474, DOI: 10.1016/j.polymer.2008.07.055.

(43) Hu, Y.; Lambert, S. M.; Soane, D. S.; Prausnitz, J. M. Double-lattice model for binary polymer solutions. *Macromolecules* **1991**, *24*, 4356–4363, DOI: 10.1021/ma00015a017.

(44) Clark, E.; Lipson, J. LCST and UCST behavior in polymer solutions and blends. *Polymer* **2012**, *53*, 536–545, DOI: 10.1016/j.polymer.2011.11.045.

(45) Andersen, G. R.; Wheeler, J. C. Theory of lower critical solution points in aqueous mixtures. *The Journal of Chemical Physics* **1978**, *69*, 3403–3413, DOI: 10.1063/1.436947.

(46) Dudowicz, J.; Freed, K. F.; Douglas, J. F. Communication: Cosolvency and conon-solvency explained in terms of a Flory-Huggins type theory. *The Journal of Chemical Physics* **2015**, *143*, 131101, DOI: 10.1063/1.4932061.

(47) Lee, B.; Graziano, G. A Two-State Model of Hydrophobic Hydration That Produces Compensating Enthalpy and Entropy Changes. *Journal of the American Chemical Society* **1996**, *118*, 5163–5168, DOI: 10.1021/ja9538389.

(48) Jeppesen, C.; Kremer, K. Single-chain collapse as a first-order transition: model for PEO in water. *Europhysics Letters (EPL)* **1996**, *34*, 563–568, DOI: 10.1209/epl/i1996-00495-1.

(49) Martin, E. W.; Holehouse, A. S.; Peran, I.; Farag, M.; Incicco, J. J.; Bremer, A.; Grace, C. R.; Soranno, A.; Pappu, R. V.; Mittag, T. Valence and patterning of aromatic residues determine the phase behavior of prion-like domains. *Science* **2020**, *367*, 694–699, DOI: 10.1126/science.aaw8653.

(50) Raos, G.; Allegra, G. Macromolecular clusters in poor-solvent polymer solutions. *The Journal of Chemical Physics* **1997**, *107*, 6479–6490, DOI: 10.1063/1.474306.

(51) Panagiotopoulos, A. Z.; Wong, V.; Floriano, M. A. Phase Equilibria of Lattice Polymers from Histogram Reweighting Monte Carlo Simulations. *Macromolecules* **1998**, *31*, 912–918, DOI: 10.1021/ma971108a.

(52) Zhang, Q.; Hoogenboom, R. Polymers with upper critical solution temperature behavior in alcohol/water solvent mixtures. *Progress in Polymer Science* **2015**, *48*, 122–142, DOI: 10.1016/j.progpolymsci.2015.02.003.

(53) Arsiccio, A.; Shea, J.-E. Protein Cold Denaturation in Implicit Solvent Simulations: A Transfer Free Energy Approach. *The Journal of Physical Chemistry B* **2021**, *125*, 5222–5232, DOI: 10.1021/acs.jpcb.1c01694.

(54) Abbott, L. J.; Stevens, M. J. A temperature-dependent coarse-grained model for the thermoresponsive polymer poly(N-isopropylacrylamide). *The Journal of Chemical Physics* **2015**, *143*, 244901, DOI: 10.1063/1.4938100.

(55) Dhamankar, S.; Webb, M. A. Chemically specific coarse-graining of polymers: Methods and prospects. *Journal of Polymer Science* **2021**, *59*, 2613–2643, DOI: 10.1002/pol.20210555.

(56) Potts, R. B. Some generalized order-disorder transformations. *Mathematical Proceedings of the Cambridge Philosophical Society* **1952**, *48*, 106–109, DOI: 10.1017/s0305004100027419.

(57) Walker, J. S.; Vause, C. A. Theory of closed-loop phase diagrams in binary fluid mixtures. *Physics Letters A* **1980**, *79*, 421–424, DOI: 10.1016/0375-9601(80)90281-9.

(58) Deshmukh, S. A.; Sankaranarayanan, S. K. R. S.; Suthar, K.; Mancini, D. C. Role of Solvation Dynamics and Local Ordering of Water in Inducing Conformational Transitions in Poly(N-isopropylacrylamide) Oligomers through the LCST. *The Journal of Physical Chemistry B* **2012**, *116*, 2651–2663, DOI: 10.1021/jp210788u.

(59) Martinez, C. R.; Iverson, B. L. Rethinking the term "pi-stacking". *Chemical Science* **2012**, *3*, 2191, DOI: 10.1039/c2sc20045g.

(60) Danielsen, S. P. O.; Semenov, A. N.; Rubinstein, M. Phase Separation and Gelation in Solutions and Blends of Heteroassociative Polymers. *Macromolecules* **2023**, *56*, 5661–5677, DOI: 10.1021/acs.macromol.3c00854.

(61) Wang, R.; Wang, Z.-G. Theory of Polymer Chains in Poor Solvent: Single-Chain Structure, Solution Thermodynamics, and Θ Point. *Macromolecules* **2014**, *47*, 4094–4102, DOI: 10.1021/ma5003968.

(62) Shultz, A. R.; Flory, P. J. Phase Equilibria in Polymer—Solvent Systems1,2. *Journal of the American Chemical Society* **1952**, *74*, 4760–4767, DOI: 10.1021/ja01139a010.

(63) Bae, Y. C.; Shim, J. J.; Soane, D. S.; Prausnitz, J. M. Representation of vapor–liquid and liquid–liquid equilibria for binary systems containing polymers: Applicability of an extended flory–huggins equation. *Journal of Applied Polymer Science* **1993**, *47*, 1193–1206, DOI: 10.1002/app.1993.070470707.

(64) Arlt, M., W.; M. E. A, P., Rasmussen; Sorensen, J. M. Liquid-Liquid Equilibrium Data Collection. *DECHEMA Chemistry Data Series, Volume V* **1979**, *86*, 761–761, DOI: 10.1002/bbpc.19820860819.

(65) Oh, S. Y.; Yang, H. E.; Bae, Y. C. Molecular simulations and thermodynamic modeling for closed-loop phase miscibility of aqueous PEO solutions. *Macromolecular Research* **2013**, *21*, 921–930, DOI: 10.1007/s13233-013-1121-7.

(66) Hansen, N.; Ostermeier, A. Completely Derandomized Self-Adaptation in Evolution Strategies. *Evolutionary Computation* **2001**, *9*, 159–195, DOI: 10.1162/106365601750190398.

(67) Jin, J.; Pak, A. J.; Durumeric, A. E. P.; Loose, T. D.; Voth, G. A. Bottom-up Coarse-Graining: Principles and Perspectives. *Journal of Chemical Theory and Computation* **2022**, *18*, 5759–5791, DOI: 10.1021/acs.jctc.2c00643.

(68) Noid, W. G. Perspective: Advances, Challenges, and Insight for Predictive Coarse-Grained Models. *The Journal of Physical Chemistry B* **2023**, *127*, 4174–4207, DOI: 10.1021/acs.jpcb.2c08731.

(69) Rekhi, S.; Sundaravadivelu Devarajan, D.; Howard, M. P.; Kim, Y. C.; Nikoubashman, A.; Mittal, J. Role of Strong Localized vs Weak Distributed Interactions in Disordered Protein Phase Separation. *The Journal of Physical Chemistry B* **2023**, *127*, 3829–3838, DOI: 10.1021/acs.jpcb.3c00830.

(70) Wadsworth, G. M.; Zahurancik, W. J.; Zeng, X.; Pullara, P.; Lai, L. B.; Sidharthan, V.; Pappu, R. V.; Gopalan, V.; Banerjee, P. R. RNAs undergo phase transitions with lower critical solution temperatures. *Nature Chemistry* **2023**, *15*, 1693–1704, DOI: 10.1038/s41557-023-01353-4.

(71) An, Y.; Webb, M. A.; Jacobs, W. M. Active learning of the thermodynamics-dynamics trade-off in protein condensates. *Science Advances* **2024**, *10*, DOI: 10.1126/sciadv.adj2448.